Fall 9-10-2018

Distribution of Knock Frewquencies in Modern Engines Compared to Historical Data

Vikram Mittal
United States Military Academy, vikram.mittal@westpoint.edu

2018-01-1666 Published 10 Sep 2018

Distribution of Knock Frequencies in Modern Engines Compared to Historical Data

Vikram Mittal US Military Academy

Citation: Mittal, V., "Distribution of Knock Frequencies in Modern Engines Compared to Historical Data," SAE Technical Paper 2018-01-1666, 2018, doi:10.4271/2018-01-1666.

Abstract

It is widely known that the rapid autoignition of end-gas will cause an engine cylinder to resonate, creating a knocking sound. These effects were quantified for a simple engine geometry in 1934 in a study where critical resonance frequencies were identified. That analysis, performed by Charles Draper, still forms the basis of most knock studies. However, the resonance frequencies are highly dependent on the engine geometry and the conditions inside the cylinder at autoignition. Since, engines and fuels operate at substantially different conditions than they did in 1934, it is expected that there should be a shift in knock frequencies. Experimental tests were run to collect knock data in an engine, representative of modern geometries, over a range of operating conditions for a number of different fuels. The operating conditions-intake air temperature, intake air pressure, and engine speed-were varied to identify shifts in the critical frequencies. Additionally, fuels were varied in octane number from 80 to 100. The resulting analysis found that the first circumferential mode, at approximately 6 kHz still played a substantial role in knock in modern engines. However, the analysis also found a decreased contribution from radial modes and an increased contribution from the axial modes. The distributions of frequencies did not shift significantly for changes in the intake air temperature or pressure; however, the axial modes became more significant at higher engine speeds. Additionally, the axial modes increase in frequency for higher octane fuels, which have an earlier knock-limited spark advance. These results show the increased importance of the axial modes in knock for modern engines; these modes are typically not audible, though they can still result in engine damage.

Introduction

Avoiding engine knock has historically been a critical constraint in the design of spark-ignition (SI) engines. Knock, a phenomenon caused by the rapid autoignition of end-gas ahead of a flame front, results in an irritable noise, with heavy knock resulting in engine damage. The autoignition process is a chemical process driven by in-cylinder physics; as such, knock tends to occur at higher in-cylinder pressures and temperatures. Since the maximum in-cylinder temperature and pressure set the Carnot efficiency for an engine, the automotive and fuel industries have conducted a substantial amount of knock research. In particular, substantial work was done in the pre-World War II era to characterize knock. This research set the stage for not only the octane number tests, which characterize the propensity of a fuel to knock, but also all subsequent knock research.

Though modern fuels and engines are substantially different from those used in the 1930s, much of the fundamental knowledge on knock has not changed. In particular, it is well established that the noise associated with knock occurs at the resonant frequencies of the engine cylinder. Charles Draper measured these frequencies in 1934, and his analysis still forms the basis for most research into knock frequencies [1]. However, these measurements were performed in a Cooperative Fuel Research (CFR) engine, which has a very different geometry than most modern SI engines. Additionally, modern engines operate at more extreme operating conditions than those used by Draper. This paper experimentally measures the knock frequencies in an SI engine representative of modern geometries. It then looks at the shift in frequencies associated with changes in engine operating conditions. The paper concludes by comparing these values to those measured by Draper and similar historic studies.

Knock in the CFR Engine and the Octane Tests

The majority of knock research has historically been conducted in the CFR Engine. The CFR Engine, which is built by Waukesha Motor Company, is a test engine used for the octane number tests. The CFR engine and the octane number tests were developed in 1928 to be the definitive system for quantifying knock [2]. As such, the CFR engine and the octane number test conditions have become the standard engine and test conditions for performing knock research.

The CFR engine has a unique design; in particular, it has a variable compression ratio, which can be increased from 4.0 to 18.0. Due to the nature of the variable compression ratio, other aspects of the engine geometry were kept fairly simple.

The engine has a flat roof with 1 intake and 1 exhaust valve. The bore is 3.250 in, and the stroke can be varied to change the compression ratio. The intake air is left at wide open throttle and includes the ability to heat the intake. Additionally, the fuel is delivered to the intake air through a carburetor. This engine design was different from engines in 1928 and is even more different from modern engines [2].

Similarly, the octane number test conditions are different from the knock-limited conditions in modern engines. The octane number tests are run at two test conditions-the research and motor octane tests. The research octane number test runs the engine at 600 rpm with an intake air temperature of 52 °C; the motor octane number test runs at 900 rpm with an intake air temperature of 149 °C. Once the engine runs at that condition, the compression ratio is increased until the engine knocks at a certain intensity, measured by a "bouncing pin." The final compression ratio is compared to a reference fuel compression ratio in which there is a knock event; this reference fuel defines the fuel's octane number. These test conditions were originally set at low speeds to reduce fuel costs and to promote autoignition events and not necessarily represent engine operating conditions [2].

Draper's Measurements in the CFR Engine

Though many knock studies have been conducted in the CFR engine at the octane number conditions, one of the most famous studies was conducted by Charles Draper in 1934. This study was a major breakthrough in the understanding of knock and was based on the development of high speed pressure transducers [1]. By measuring the frequency of the pressure oscillations in a knocking engine, he was able to deduce the underlying mechanism for knock. In particular, he identified that the noise associated with knock comes from the excitation of in-cylinder resonation frequencies.

In his analysis, Draper calculated out the different resonant frequencies for a perfect cylinder; he found that these values aligned with the values measured in his experiments. His analysis started with the wave equation as shown in Equation 1.

$$\nabla^2\Phi = \frac{1}{c^2}\frac{\partial^2\Phi}{\partial t^2} \quad where \quad c = \sqrt{\gamma RT} \tag{1}$$

In Equation 1, Φ is the in-cylinder acoustic pressure, c is the speed of sound, γ is the ratio of specific heats, R is the universal gas constant, and T is the in-cylinder temperature. Equation 1 can be solved in cylindrical coordinates with Dirichlet boundary conditions to get Equation 2, where n is a nodal frequency, g is an integer constant related to the axial dimension, β is a constant based on the radial dimension, and h is the height of the cylinder.

$$n = c\sqrt{\frac{\beta^2}{4\pi^2} + \frac{g^2}{4h^2}} \quad where\ g = 0,1,2 \tag{2}$$

The value for β is inversely proportional to the bore of the engine and is only allowed to have certain values. Draper then gives the following six values for the product of β and the bore: 3.82, 7.01, 10.30, 1.84, 5.33, and 8.53.

Equation 2 show that the knocking frequencies are based on the engine design and operating conditions, which set the relevant length scales and the speed of sound. The speed of sound is determined by the in-cylinder temperature at knock onset which is a function of the engine operating condition and the fuel.

Draper proceeds to set the value of g to 0, removing the axial modes for the remainder of his analysis. Draper justifies this assumption since the cylinder height close to TDC is much less than the cylinder bore in a CFR Engine. With g set to 0, Draper proceeded to measure the six frequencies shown in Figure 1 that align with the frequencies determined from the wave equation. These six radial and circumferential frequencies are between 6.2 and 18 kHz.

Figure 2 gives the frequency distribution for the MON80 and MON85 tests (right), along with a representative pressure trace (left). This data was provided by Waukesha and is similar to the conditions used by Draper [1]. The frequency distribution was calculated by taking the Fourier Transform for 100 knocking cycles. The cycle shows that the trough-to-crest amplitude of the knocking signal is 15 bar, which corresponds to heavy knocking conditions. Audible knock can occur when this amplitude is well below 1 bar [3]. Additionally, knock occurs early in the engine cycle, with the oscillations starting prior to top dead center (TDC).

The frequency distribution shows that there are five ranges of excited frequencies, corresponding to the frequencies shown in Figure 1. The largest contribution comes from the first circumferential mode at 6 kHz. There is a lesser contribution from the higher frequencies that are between 10 and 18 kHz.

Multiple knock studies have been performed to analyze the excited frequencies for SI engines. These studies typically assume that the axial modes are not excited; therefore, they are left out of their analyses [4, 5, 6, 7, 8, 9]. These studies trace this assumption back to Draper's assumption for the

FIGURE 1 Radial and circumferential modes excited by autoignition calculated by Draper in the CFR Engine and the associated values for the test engine.

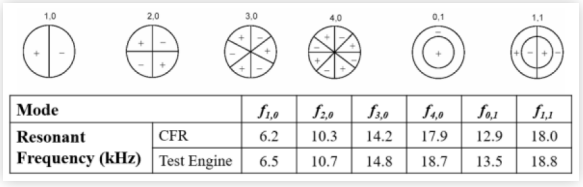

Mode		$f_{1,0}$	$f_{2,0}$	$f_{3,0}$	$f_{4,0}$	$f_{0,1}$	$f_{1,1}$
Resonant Frequency (kHz)	CFR	6.2	10.3	14.2	17.9	12.9	18.0
	Test Engine	6.5	10.7	14.8	18.7	13.5	18.8

FIGURE 2 Pressure trace for a typical cycle for a CFR engine operating at the MON80 test conditions.

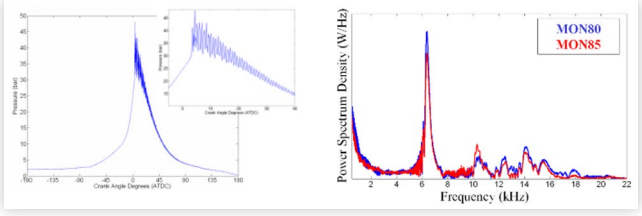

CFR engine. Additionally, since the knock frequencies associated with the axial mode are above the threshold of human hearing, typically 10 kHz, they would be irrelevant for studies concerned with knock as a noise [5].

Knock in Modern Engines

Modern engines have a different engine geometry and operate at different conditions than those used by Draper. The CFR Engine has a pancake shaped combustion chamber. Meanwhile, modern engines tends to have more complex geometries, the most common being a pent-roof geometry. Both engine geometries are depicted in Figure 3. Most engine geometries have similar bores due to heat transfer optimization constraints. For the CFR engine in the octane number tests (MON80), the axial distance between the cylinder head and the piston at knock onset is approximately 20 mm. Modern engines have combustion chamber shaped like a pent-roof and have a distance generally greater than 30 mm. While a flat cylindrical combustion chamber would be expected to excite the circumferential modes, which are related to the bore of the engine, a more complex geometry is likely to excite multiple other frequencies as well. Additionally, the larger axial distances would likely result in the excitation of axial modes. Due to the complex geometry of modern engines, the resonance frequencies cannot be readily calculated. Several studies have used finite element modeling to determine the resonant frequencies. These studies have different results based on the assumptions of the models; however, they all have the first circumferential mode at approximately 6 kHz and a range of higher frequencies between 15 and 25 kHz [10, 11].

Moreover, modern engines operate at conditions substantially different from those used by Draper, who set the engine test conditions to coincide with the octane number tests. The octane number tests are run at lower speeds and higher intake air temperatures than modern engines. Additionally, the tests were run with lower octane number fuels than modern engines, resulting in lower compression ratios in the test.

These changes in engine operating conditions effect the engine geometry when knock occurs, as captured in the Livengood-Wu autoignition integral displayed in Equation 3 [12, 13]. Equation 3 shows the autoignition integral; the integral spans from the closing of the intake air valve and continues until all the fuel combusts.

FIGURE 3 Cross section of the engine geometries for a modern pent-roof engine (top) and the CFR engine (bottom) at 10 degrees after top dead center.

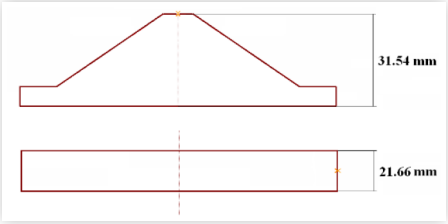

$$I = \int_0^{t'} \frac{dt}{\tau_i(T,P)} \tag{3}$$

In Equation 3, if the value of I reaches 1, an autoignition event occurs. The variable τ is the autoignition delay time, which is a function of in-cylinder temperature (T) and pressure (P). The autoignition delay time decreases with higher temperatures and pressures, consistent with most exothermic chemical processes.

Based on Equation 3, slower engine speeds allows more time for the autoignition event to occur resulting in autoignition occurring earlier in the engine cycle. Additionally, hotter intake air temperatures will result in autoignition occurring earlier. These trends are visible in Figure 2, where the knocking event occurs earlier in the engine cycle than when knock would occur in most modern engines.

Since knock occurs close to TDC in Draper's tests, the axial length scales are small compared to the radial and circumferential length scales. The smaller length scale results in very high frequencies that were disregarded in his experiments and analysis. However, the pent-roof geometry, coupled with a later knocking event makes the axial lengths scales comparable to the radial and circumferential length scales. With comparable length scales, it would be expected that the axial modes are more likely to be excited.

Effects of Engine Operating Conditions on Knock Frequencies

Experimental Setup Knock data was collected for a number of fuels at a number of engine operating conditions. The data was collected on a single-cylinder test engine-a Ricardo MK III base with a Volvo B5254 pent-roof, 4-valve, central spark plug cylinder head. The engine has a compression ratio of 9.8 which is consistent with compression ratios for modern SI engines [14]. At maximum brake torque timing, wide open throttle, and stoichiometric conditions, the engine has a mean effective pressure of 10.2 bar. Other engine parameters are given in Table 1.

The test engine was outfitted with a Kistler 6125A pressure transducer. The pressure transducer sampled at 90 kHz, equivalent to 10 samples per crank angle degree for an engine running at 1500 rpm. The pressure transducer response is fast enough to pick up a large range of oscillations from knock.

TABLE 1 Specifications for test engine used in this study

Parameter	Value
Bore	83 mm
Stroke	90 mm
Connecting Rod Length	158 mm
Displaced Volume	487 cc
Clearance Volume	55 cc
Compression Ratio	9.8:1
Intake Valve Opening/Closing	0° BTC, 60° ABC
Exhaust Valve Opening/Closing	48° BBC, 12° ATC

The data was logged using a National Instruments 6023E data acquisition card.

The complex geometry would necessitate a finite element model to determine the resonant frequencies; however, the frequencies can be approximated through Draper's analysis. These frequencies are shown in Figure 1. Note that these frequencies ignores the contributions from the axial modes.

The engine was set to run at a given condition with the spark retarded to ensure no knock. The spark was then advanced in 1° increments until the engine audibly knocked. This spark timing is considered the knock limited spark advance (KLSA). The pressure traces were visible on an oscilloscope to ensure that the engine was knocking. The spark was advanced 2° past knock onset into a heavy knocking regime. At this condition, 1000 cycles of data was collected.

After the data was collected, each engine cycle was isolated and a Fast Fourier Transform (FFT) was performed on that cycle. The FFT for each cycle was then summed and normalized over the 1000 cycles to minimize the effects of cycle-to-cycle variation. The FFT identifies the frequencies that the in-cylinder pressure waves are oscillating at. The FFT for a knocking and a non-knocking condition is shown in Figure 4.

Though the bulk of knock frequency studies focus on an individual engine operating condition, knock frequencies are expected to shift with operating conditions. Therefore, three parameters were selected to vary in the design of experiment - engine speed, intake air temperature, and boosting level. A base testing condition was defined as 1500 rpm, 25 °C intake air temperature, and no boosting. This base condition was selected to correspond to a knock-limited operating condition for modern engines and fuels. Each parameter was individually varied from the base condition to look at the effects of changing the operating condition on the excited knock frequency. Table 2 displays the different operating conditions that were tested.

Initial tests found that the frequency spectrums varied based on the KLSA which was based on the fuel and the operating conditions. To minimize these effects, the fuels were varied to maintain a consistent KLSA of 5° BTDC. The bulk of the fuels used were Primary Reference Fuels (PRFs), which are blends of iso-octane and n-heptane. A PRF typically has a numerically designation associated with the octane number of the blend. Additionally, Universal Test Gasolines (UTG) were used, which similarly have numerical designations

FIGURE 4 Frequency distribution for a knocking test condition (blue) and a not-knocking test condition (red).

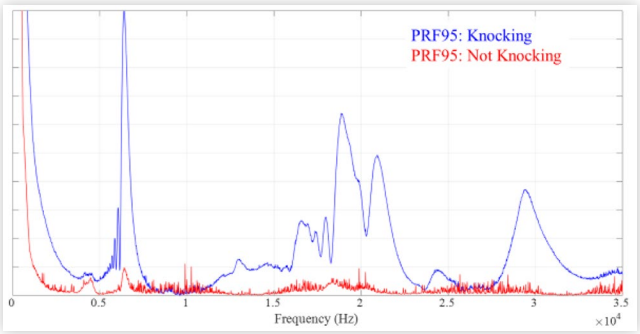

TABLE 2 Engine operating conditions that were tested as part of this study

Fuel	Engine Speed (RPM)	Intake Air Temperature (°C)	Boosting
PRF95	1500	30	0%
PRF90, PRF100, UTG96, Cyclopentene	1500	30	0%
PRF90	2500	30	0%
UTG96	1500	50	0%
Toluene Blend	1500	70	0%
UTG96	1500	30	20%
Toluene Blend	1500	30	40%

associated with their octane number. A few other fuels were used including cyclopentene and toluene blends.

Effects of Spark Timing on Knock Frequencies

The test engine was run at the base test condition with UTG96 to identify the different knocking frequencies. The tests were repeated with cyclopentene, both of which have a KLSA of 5° before TDC. The frequency distributions for the two tests are shown in Figure 5. This figure shows little variation in the frequencies excited, as would be expected since the engine geometries at knock onset would be similar. Fuels with different KLSA were also tested. The results for PRF90, PRF95, and PRF100 are shown in Figure 6.

Three ranges of frequencies can readily be identified from the frequency distributions. The first frequency range is between 6 and 7 kHz. This frequency was also found by Draper and most historic studies. This frequency band corresponds to the first circumferential mode, which is based on the bore of the engine. Since the engine bore is independent of piston position, there was no notable shift in that frequency band with a change in KLSA.

The second frequency range is between 15 and 23 kHz, which is above the human hearing threshold. However, since the amount of energy released scales with the integral of the FFT, the results show that a large amount of the energy is released by the autoignition process in this frequency domain. This frequency domain consists of multiple bands

FIGURE 5 Frequency distribution of heavy knock conditions for engine at base operating condition (1500 rpm, WOT, 25 °C intake air temperature) for different fuels with similar knock limited spark advance.

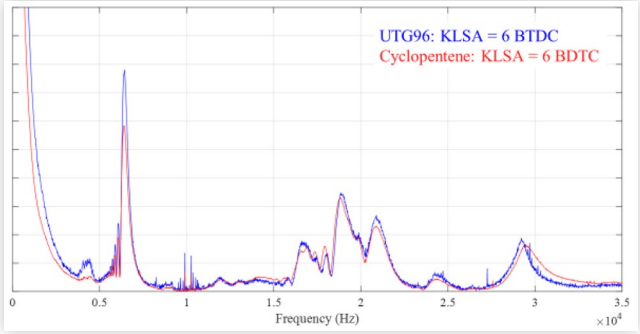

FIGURE 6 Frequency distribution of heavy knock conditions for engine at base operating condition (1500 rpm, WOT, 25 °C intake air temperature) for different fuels with different knock limited spark advances.

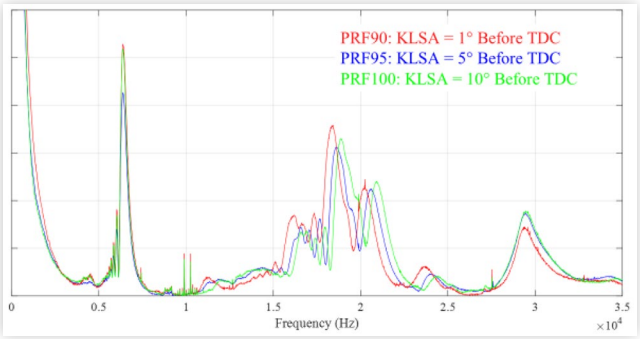

FIGURE 7 Frequency distribution of heavy knock conditions for engine at different speeds (WOT, 25 °C intake air temperature). Higher octane fuel was used for the slower speed to maintain the same knock limited spark advance.

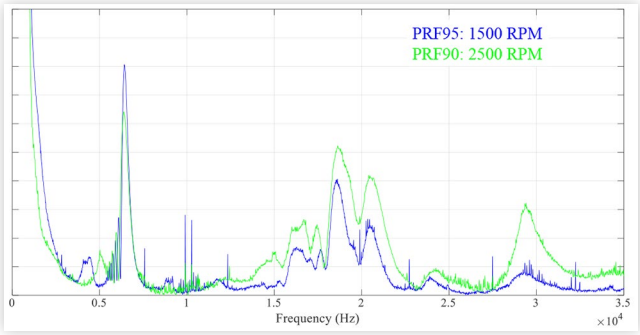

of frequencies. The two main frequency band are 18 to 20.5 kHz and 20.5 to 23 kHz, both of which were not found in Draper analysis. A shift is noticeable in these frequencies with KLSA. Since autoignition occurs as the piston is moving downwards, an earlier KLSA correlates to knocking occurring earlier in the cycle, such that there is a shorter distance between the roof of the chamber and the piston head. As such, the higher octane fuels, which have an earlier KLSA, would have a higher frequency. The shift in frequencies with the KSLA and the broad distributions indicate that these frequencies are related to the axial modes.

The third frequency range is between 28 and 32 kHz. This frequency range is fairly broad although it only encompasses one band of frequencies. These frequencies were also not found by Draper. Though the broad distribution indicates that it could be an axial mode, there is no shift with the KLSA. It is likely a mode that relates to the width of the top of the cylinder head, which is approximately 20% of the bore. Since the first circumferential frequency, which scales with the bore of the engine, is at 6 kHz, the associated frequency associated with the top of the pent-roof should be approximately 30 kHz.

Effects of Speed on Knock Frequencies Draper measured the knock frequency in accordance with the octane tests, which are at 600 and 900 rpm; however, modern engines do not even idle at speeds that low. Knock data was collected and analyzed at different engine speeds to capture the effects of engine speed on knock frequencies. Increased engine speeds result in an earlier KLSA, which can cause a shift in the higher frequencies, as previously discussed. Therefore, this analysis uses different fuels in order to keep a consistent KLSA. The test engine was run at 1500 rpm and 2500 rpm with PRF100 and PRF95 respectively; the frequency distributions are shown in Figure 7.

This increase of contributions from higher frequency modes is likely due to the motion of the piston. Since the piston is moving in the axial direction, the faster speeds could excite the axial modes.

Effects of Intake Air Temperature on Knock Frequencies The test engine was run at different intake air temperatures to identify the different knocking frequencies. Increasing the intake air temperature results in a fuel having a later KLSA, which can cause a change in the high frequencies, as shown in Figure 5. To isolate the effects of temperature from the change in the KLSA, higher octane fuels were used for the higher temperature tests, such that all the tests maintain a KLSA of 5° before TDC. The test engine was run with PRF95 with no heating of the intake; UTG96 with a 20 °C increase in the intake air temperature; and a toluene blend with a 40 °C increase in the intake air temperature. The frequency distributions are shown in Figure 8.

Though the intake air temperature is increased, the in-cylinder temperatures at autoignition only change by a small amount. The large temperature rise comes from the energy released by the fuel, dwarfing the effects of heating the intake air temperature.

The frequency distributions show a small shift in the frequencies, especially at the higher frequencies. A change in intake air temperature of 40 °C results in the speed of sound at knock onset increasing by approximately 3.0 percent. The frequency distribution shows a shift of approximately 1.7 percent. Though the frequency shift is not as large as theoretically calculated, some of the impacts of the increased air temperature are reduced by heat transfer effects.

FIGURE 8 Frequency distribution of heavy knock conditions for engine at different intake air temperatures (WOT, 1500 rpm). Higher octane fuel was used for the higher temperatures to maintain the same knock limited spark advance.

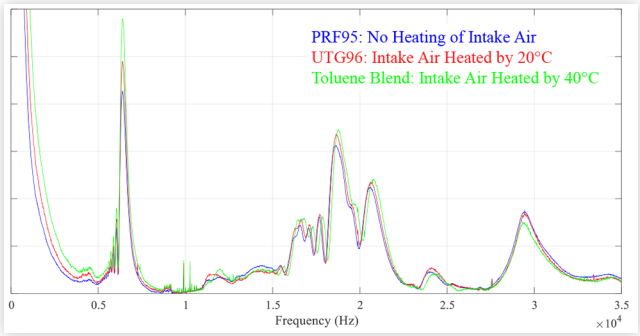

FIGURE 9 Frequency distribution of heavy knock conditions for engine at different boosting levels (25 °C intake air temperature, 1500 rpm). Higher octane fuel was used for the higher boosting levels to maintain the same knock limited spark advance.

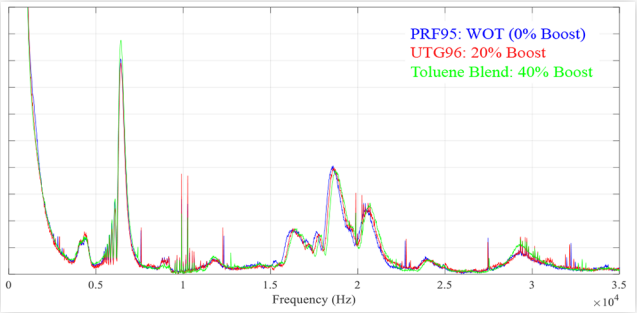

The frequency distributions show that as the intake air is heated, there is an increased contribution from the first circumferential mode at 6 kHz over the higher frequencies. This increase can be seen in the results presented by Eng, where the intake air was heated to 90 °C [4].

Effects of Boosting on Knock Frequencies Based on the wave equation, it is expected that the knock frequencies will not change based on the intake air pressure, aside from the change in engine geometry related to changes in the KLSA. Data was collected with the engine at 0 percent, 20 percent, and 40 percent boost levels. Fuels were selected to keep a constant knock-limited spark advance. The wide-open throttle data was collected with PRF95, the 20 percent boosting data was collected with UT96, and the 40 percent boosting data was collected with a toluene blend.

The frequency distribution is shown in Figure 9. No shift in knock frequencies were noted by changes in boosting levels. This trend is expected from the wave equation, where the frequency is based on the speed of sound, which is independent of the in-cylinder pressure.

Comparison between Historic Knock Data and Experimental Results

Overall the data collected and analyzed in the previous section did not show a significant shift in frequencies with operating conditions. The frequencies were dependent on the KLSA, especially the higher frequencies. However, different fuels with the same KLSA had comparable frequency spectrums. A small increase was found for the higher frequency band as the intake air temperature increases. Additionally, the frequency contribution was stronger for the higher frequency ranges as the engine speed increased. Boosting did not have a significant impact.

The experimental data for the base test condition (1500 rpm, WOT, 25 °C intake air temperature, UTG96) was compared to the frequencies measured in the MON80 test, which aligns with Draper's analysis and several historic studies.

TABLE 3 Contribution from different frequency bands for knock in the CFR Engine and the modern engine

Frequency Range (kHz)	Knock in CFR Engine (%)	Knock in Modern Engine (%)
6.0-7.8	48	20
10.0-11.2	15	2
12-13.1	9	3
13.8-15.0	14	4
15.0-16.2	8	10
17.8-18.2	2	5
18.2-20.5	0	19
20.5-22.0	0	17
23.7-25.5	0	4
27.5-31.5	0	12

The frequency spectrum plot was integrated over each frequency band to calculate the percent contribution from a given band. The results are shown in Table 3.

The first circumferential mode (6.0-7.8 kHz) is seen as being relevant for both test conditions. Since the first circumferential mode is based on the bore of the engine, and both engines have comparable bores, it follows that the frequencies would be similar. A small increase in frequency can be observed for the modern engine; it is due to modern engines running at hotter temperatures than those used by the octane tests.

The tests found a substantial shift in the higher frequencies. These changes likely occur for the following reasons:

1. Modern engines have a pent-roof design resulting in larger axial length scales, which result in lower frequencies that are more substantial.
2. Knock occurs closer to TDC in the Octane Number tests, resulting in a smaller axial length scale, especially when compared to the circumferential length scales. As such, the axial frequencies could be neglected. However, knock in modern engines occurs several degrees after TDC, resulting in a larger axial length scale.
3. The pent-roof geometry results in the radial frequencies being negligible in modern engines.
4. The complex geometry associated with the pent-roof design results in more frequency bands over a larger range being excited.

Of interest is that modern engines tend to have higher frequencies excited than those in the octane tests. Though these frequencies are above the audible range, they could still cause the engine cavity to resonate at audible frequencies. Engine damage through knock is typically caused through damage to the piston rings or the cylinder bore. These damage mechanisms are more likely to occur from knock at higher frequencies [15].

Conclusions and Future Work

Since the invention of the automobile, knock has been a critical design issue for internal combustion engines. Much

of knock knowledge is based on data collected in the CFR engine under octane number test conditions. In particular, a major study by Draper in 1934 set the stage for most future knock research; that study found that knock frequencies aligned with the resonant frequencies of the engine cylinder. This study also found that the axial modes were not excited, an assumption that prevailed in numerous subsequent studies.

Since the resonance frequencies are highly dependent on engine geometry and operating conditions, knock data was collected in a modern engine at standard operating conditions. The results found that the first circumferential mode, approximately 6 kHz, has a large contribution in modern engines, similar to what was found by Draper. However, other frequency ranges are substantially different. These differences are caused by the change in engine geometry, primarily the incorporation of pent-roof heads over flat heads. This geometry results in an increased excitation of the axial modes. As a result there is a significant contribution from high frequencies that are commonly neglected. Though these frequencies are not in the audible range, they can lead to engine damage.

Future work will involve looking at other engine geometries. In particular, it would identify the possibility of reducing audible knock by changing the geometries and operating conditions, allowing for knock to occur at frequency bands above the audible range.

References

1. Draper, C.S., "The Physical Effects of Detonation in a Closed Cylindrical Chamber," National Advisory Committee for Aeronautics Report Number 493, 1934.
2. Mittal, V., "The Development of the Octane Number Tests and their Impact on Automotive Fuels and American Society," *International Journal for the History of Engineering & Technology* 86, 2016, doi:10.1080/17581206.2016.1223940.
3. Mittal, V., Revier, B., and Heywood, J., "Phenomena that Determine Knock Onset in Spark-Ignition Engines," SAE Technical Paper 2007-01-0007, 2007, doi:10.4271/2007-01-0007.
4. Eng, J.A., "Characterization of Pressure Waves in HCCI Combustion," SAE Technical Paper 2002-01-2859, 2002, doi:10.4271/2002-01-2859.
5. Hickling, R. and Kamal, M., "Engine Noise: Excitation, Vibration, and Radiation," *International Symposium on Engine Noise*, Plenum Press, 1982.
6. Lee, J., Hwang, S., Lim, J., Jeon, D. et al., "A New Knock-Detection Method using Cylinder Pressure, Block Vibration and Sound Pressure Signals from a SI Engine," SAE Technical Paper 981436, 1998, doi:10.4271/981436.
7. Brunt, M., Pond, C., and Biundo, J., "Gasoline Engine Knock Analysis using Cylinder Pressure Data," SAE Technical Paper 980896, 1998, doi:10.4271/980896.
8. Szwaja, S. and Bhandary, K.R., "Comparisons of Hydrogen and Gasoline Combustion Knock in a Spark Ignition Engine," *International Journal of Hydrogen Energy* 32, 2007, doi:10.1016/j.ijhydene.2007.07.063.
9. Chen, L., Li, T., Yin, T., and Zheng, B., "A Predictive Model for Knock Onset in Spark-Ignition Engines with Cooled EGR," *Energy Conversion and Management* 87, 2014, doi:10.1016/j.enconman.2014.08.002.
10. Scholl, D., Davis, C., Russ, S., and Barash, T., "The Volume Acoustic Modes of Spark-Ignited Internal Combustion Chambers," SAE Technical Paper 980893, 1998, doi:10.4271/980893.
11. Wang, Z., Liu, H., and Reitz, R.D., "Knocking Combustion in Spark-Ignition Engines," *Progress in Energy and Combustion Science* 61, July 2017.
12. Livengood, J. and Wu, P., "Correlation of Autoignition Phenomena in Internal Combustion Engines and Rapid Compression Machines," *Symp Int Combust*, 1955.
13. Kalghatgi, G. and Bradley, D., "Pre-Ignition and 'Super Knock' in Turbo-Charged Spark-Ignition Engines," *Int J Engine Res* 13(4):399-414.
14. Ward's Automotive Group Databases: Light Vehicle Engines, North American Availability and Specifications for 2017.
15. Nates, R. and Yates, A., "Knock Damage Mechanisms in Spark-Ignition Engines," SAE Technical Paper 942064, 1994, doi:10.4271/942064.

Contact Information

The main author can be contacted by e-mail at vikram.mittal@usma.edu

Acknowledgments

The experimental data was collected as part of the author's doctoral thesis at the Massachusetts Institute of Technology. The research was funded by the Engine and Fuels Consortium, consisting of General Motors, Chrysler, Ford Motor Company, Royal Dutch Shell, and Saudi Aramco.

Definitions/Abbreviations

WOT - Wide Open Throttle

KLSA - Knock-limited spark advance

TDC - Top Dead Center

CFR - Cooperative Fuel Research

PRF - Primary Reference Fuel

UTG - Unleaded Test Gasoline

ON - Octane Number

RPM - Revolutions per minute

ISSN 0148-7191